Available online at www.sciencedirect.com
SCIENCE DIRECT®
ELSEVIER
International Journal of Engineering Science 42 (2004) 509–519
International Journal of Engineering Science
www.elsevier.com/locate/ijengsci

Hydromagnetic squeezed flow and heat transfer over a sensor surface

A.-R.A. Khaled [a], K. Vafai [b,*]

[a] Department of Mechanical Engineering, The Ohio State University, Columbus, OH 43210, USA
[b] Department of Mechanical Engineering, University of California, A363 Bourns Hall, Riverside, CA 92521-0425, USA

Received 14 June 2003; received in revised form 27 July 2003; accepted 15 August 2003

(Communicated by G. AHMADI)

Abstract

Hydromagnetic effects are analyzed on flow and heat transfer over a horizontal surface placed in an externally squeezed free stream. The unsteady governing momentum and energy equations are transformed to similarity equations for certain families of the controlling parameters. It is found that both local wall shear stress and local Nusselt number increase as squeezing free stream velocity increases. Also, local Nusselt number is found to increase by an increase in the magnetic parameter. Further, the local wall shear stress is observed to increase as the magnetic parameter increases. Finally, hydromagnetic and suction wall permeable velocity (for permeable surfaces) effects are found to enhance the temperature or the concentration near the sensor surface. Thus, they enhance the detection capability of the sensor as long as the chemical binding at the sensor surface is not suppressed by increases in flow associated with these effects.

Keywords: Hydromagnetic; Sensor surface; Similarity; Squeezed flow; Unsteady

1. Introduction

Many chemical and biological sensors involve extending surfaces as their sensing elements. An example of these elements is the microcantilever [1] which has the advantage to accurately sense various diseases or can be used to detect many hazardous or bio-warfare agents. The microcantilever bends upon the binding of the target molecules with the receptor coating on one of its

* Corresponding author. Tel.: +1-909-787-2135; fax: +1-909-787-2899.
E-mail address: vafai@engr.ucr.edu (K. Vafai).

0020-7225/$ - see front matter
doi:10.1016/j.ijengsci.2003.08.005

Nomenclature

a	squeeze flow strength
B_{m}	strength of the magnetic field
B_{mo}	reference strength of the magnetic field
b	index of the squeeze flow
f	transformed stream function
f_0	dimensionless permeable velocity
h	height of the channel
h_{c}	convective heat transfer coefficient
k	fluid thermal conductivity
N	dimensionless magnetic parameter
Nu	Nusselt number
Pr	fluid Prandtl number
p	fluid pressure
q	heat flux
q_0	reference heat flux
Re	free stream Reynolds number
T	temperature
T_∞	free stream temperature
t	time
U	free stream velocity
u	dimensional axial velocity
v	dimensional normal velocity
v_0	surface dimensional permeable velocity
v_i	reference surface permeable velocity
x	axial distance
y	normal distance

Symbols

α	fluid thermal diffusivity
η	similarity transformation in terms of y and t
μ	fluid dynamic viscosity
θ	transformed fluid temperature
ρ	fluid density
σ_{m}	electrical conductance of the fluid
υ	fluid kinematic viscosity
ψ	stream function

surfaces. The microcantilever is usually placed in thin film fluidic cells which can be subject to relatively large level of external squeezing in the presence of external disturbances. The flow over the microcantilever can be modeled as flow over a horizontal surface.

The effect of magnetic field normal to the flow of an electrically conducting fluid on the boundary layer over a horizontal surface is widely discussed in the literature (e.g. [2,3]). Recently, the effects of magnetic field on oscillatory squeezed flows has been studied inside thin films by Khaled and Vafai [4] where they show that magnetic field can reduce flow instabilities inside thin films associated with large squeezing effects. However, the literature lacks studies about the effects of the magnetic field on flow and consequently on heat and mass transfer over a sensor surface placed inside fluidic cells subject to squeezed flow conditions.

In this work, hydromagnetic effects are considered on dynamical and thermal boundary layer characteristics over a horizontal permeable surface in the presence of specified unsteady external squeezing flows. The analysis is concerned with certain family of squeezed flows such that the resulting flows can be solved using similarity transformation.

2. Problem formulation

Consider flow over a horizontal surface. The surface is assumed to have a length L. The x-axis is taken along the length of the surface starting from its free end while the y-axis is taken normal to the upper surface as shown in Fig. 1. The surface is enclosed inside a squeezed channel such that the height $h(t)$ is much greater than the boundary layer thickness and the squeezing in the free stream is assumed to start from the tip of the surface as illustrated in Fig. 1. This problem can find its application in flow over microcantilever sensor caused by an external squeezing at the boundaries of the fluidic cell.

The working fluid is taken to be Newtonian and electrically conducting with σ_m as its electrical conductance. It is assumed that a magnetic field with a time-dependent strength B_m is applied normal to the flow in the y-direction and that the induced magnetic Reynolds number is negligible. The continuity, momentum and energy governing equations are

$$\frac{\partial u}{\partial x}+\frac{\partial v}{\partial y}=0 \tag{1}$$

$$\frac{\partial u}{\partial t}+u\frac{\partial u}{\partial x}+v\frac{\partial u}{\partial y}=-\frac{1}{\rho}\frac{\partial p}{\partial x}+\upsilon\frac{\partial^2 u}{\partial y^2}-\frac{\sigma_m B_m^2}{\rho}u \tag{2}$$

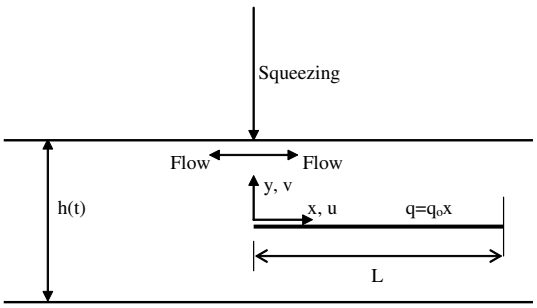

Fig. 1. Schematic diagram.

$$\frac{\partial U}{\partial t} + U\frac{\partial U}{\partial x} = -\frac{1}{\rho}\frac{\partial p}{\partial x} - \frac{\sigma_m B_m^2}{\rho}U \tag{3}$$

$$\frac{\partial T}{\partial t} + u\frac{\partial T}{\partial x} + v\frac{\partial T}{\partial y} = \alpha\frac{\partial^2 T}{\partial y^2} \tag{4}$$

where u, v, U, T, t and α are the axial component of the velocity, normal component of the velocity, axial free stream velocity, temperature, time and thermal diffusivity of the working fluid, respectively. The fluid pressure is p while υ is the kinematic viscosity of the fluid. Eqs. (2) and (4) are applicable within the boundary layer while Eq. (3) governs the outer stream flow which is assumed to be invisid and uniform with respect to the normal coordinate. The error associated with this assumption is minimized when the sensor length is taken to be much smaller than the channel height. Eq. (2) is transferred to the following after eliminating the pressure gradient using Eq. (3):

$$\frac{\partial u}{\partial t} + u\frac{\partial u}{\partial x} + v\frac{\partial u}{\partial y} = \frac{\partial U}{\partial t} + U\frac{\partial U}{\partial x} + \upsilon\frac{\partial^2 u}{\partial y^2} + \frac{\sigma_m B_m^2}{\rho}(U-u) \tag{5}$$

A generalized set of boundary conditions are imposed

$$u(x,0,t) = 0 \quad v(x,0,t) = v_0(t) \quad u(x,\infty,t) = U(x,t) \tag{6a,b,c}$$

$$-k\frac{\partial T(x,0,t)}{\partial y} = q(x) \quad T(x,\infty,t) = T_\infty \tag{6c,d}$$

where T_∞, $U(x,t)$ and $q(x)$ are the free stream temperature, free stream velocity and the wall heat flux, respectively. It is assumed that wall heat flux is a prescribed function of the axial distance x. The reference velocity $v_0(t)$ represents the velocity at the sensor surface when permeable surfaces are considered. This velocity is proportional to the normal velocity at the disturbed boundary and it increases as sizes of the surface pores increase or when the surface is placed close to the disturbed boundary. Eqs. (4) and (5) can be transformed to similarity equations when the following variables and conditions are implemented:

$$U = ax \quad \eta = y\sqrt{\frac{a}{\upsilon}} \quad a = \frac{1}{s+bt} \tag{7a,b,c}$$

$$f(\eta) = \frac{\psi}{x\sqrt{a\upsilon}} \quad \theta(\eta) = \frac{T-T_\infty}{\frac{q_0 x}{k}\sqrt{\frac{\upsilon}{a}}} \quad q(x) = q_0 x \tag{7d,e,f}$$

$$B_m(t) = B_{mo}\sqrt{a} \quad v_0(t) = v_i\sqrt{a} \tag{7g,h}$$

where b and s are arbitrary constants. The parameters a, q_0 and k are the strength of squeeze flow, reference wall heat flux and the thermal conductivity of the fluid, respectively. Conditions 7(a) and 7(c) reveal that the motion of the channel's height is governed by the following relation:

$h(t) = h_0/(s+bt)^{(1/b)}$ for $b > 0$ and $h(t) = h_0 e^{-st}$ for $b = 0$ where h_0 is a constant. The variable ψ represents the stream function while f is the transformed stream function. When mass transfer is considered, it can be assumed that the wall mass flux will have a trend similar to that for the wall heat flux. Accordingly, the transformed species concentration will have a similar trend to that for the transformed temperature θ. The constants B_{mo} and v_i are a reference magnetic field and a reference suction velocity, respectively. The restricted magnetic field can physically represent a magnetic source with decaying strength. The surface permeable velocity is expected to increase as the time decreases (when $b > 0$) since squeezing velocities increase as time decreases. The results of transformations of Eqs. (4) and (5) are the following similar equations:

$$f''' + \left(f + \frac{b\eta}{2}\right) f'' - (f' - b + N) f' + (1 - b + N) = 0 \tag{8}$$

$$\frac{1}{Pr}\theta'' + \left(f + \frac{b\eta}{2}\right)\theta' - \left(f' + \frac{b}{2}\right)\theta = 0 \tag{9}$$

where Pr is the Prandtl number ($Pr = \upsilon/\alpha$). The prime denotes the derivative with respect to η. The corresponding transformed boundary conditions are

$$f'(0) = 0 \quad f(0) = -f_0 \quad f'(\infty) = 1 \tag{10a,b,c}$$

$$\theta'(0) = -1 \quad \theta(\infty) = 0 \tag{10d,e}$$

According to conditions 7(g) and 7(h), the parameters N and f_0 appearing in Eq. (8) and 10(b) are constants and they are equal to

$$N = \frac{\sigma_{\mathrm{m}} B_{\mathrm{mo}}^2}{\rho} \quad f_0 = \frac{v_i}{\sqrt{\upsilon}} \tag{11a, b}$$

The parameter N represents the dimensionless magnetic parameter while f_0 represents the dimensionless permeable velocity parameter. In absence of hydromagnetic and wall permeable velocity effects, Eqs. (8–10) reduce to the following similar equations with a fewer restricted condition:

$$f''' + \left(f + \frac{b\eta}{2}\right) f'' - (f' - b) f' + (1 - b) = 0 \tag{12}$$

$$\frac{1}{Pr}\theta'' + \left(f + \frac{b\eta}{2}\right)\theta' - \left(f' + \frac{b}{2}\right)\theta = 0 \tag{13}$$

$$f(0) = f'(0) = 0 \quad f'(\infty) = 1 \tag{14a,b}$$

$$\theta'(0) = -1 \quad \theta(\infty) = 0 \tag{14c,d}$$

The dimensionless local wall shear stress τ^* and the local Nusselt number Nu can be calculated from the following:

$$\tau^* = \frac{\tau_w}{\mu a Re^{1/2}} = f''(0) \quad Re = \frac{ax^2}{\upsilon} \quad Nu = \frac{h_c x}{k} = \frac{x}{\theta(0)}\sqrt{\frac{a}{\upsilon}} \tag{15a,b,c}$$

where μ, τ_w, h_c and Re are the dynamic viscosity of the fluid, wall shear stress, convective heat transfer coefficient and the free stream Reynolds number, respectively. By analogy between heat and mass transfer, Eqs. (9) or (13) can be used to govern the transport of species taking into account that θ and Pr are replaced by the corresponding transformed concentration and the Schmidt number ($Sc = \upsilon/D$, $D =$ species mass diffusivity).

3. Numerical method

Eqs. (8) and (9) were descritized using three points center differencing. The resulting tri-diagonal system of algebraic equations was then solved using the well-established Thomas Algorithm [5]. Iterations were implemented in the solution of Eq. (8) because the second and third terms of this equation are non-linear. The values of 0.0015 and 10^{-7} were selected for $\Delta\eta$ and the convergence criteria for the maximum difference for f' between the two consecutive iterations.

4. Discussions of the results

Figs. 2 and 3 show the effect of the dimensionless magnetic parameter N on velocity and temperature profiles over a horizontal surface inside squeezed free stream, respectively. It is

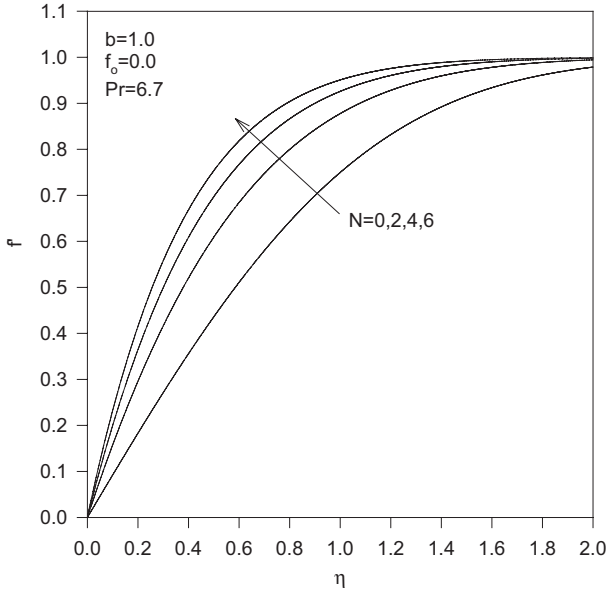

Fig. 2. Variations of f' with N.

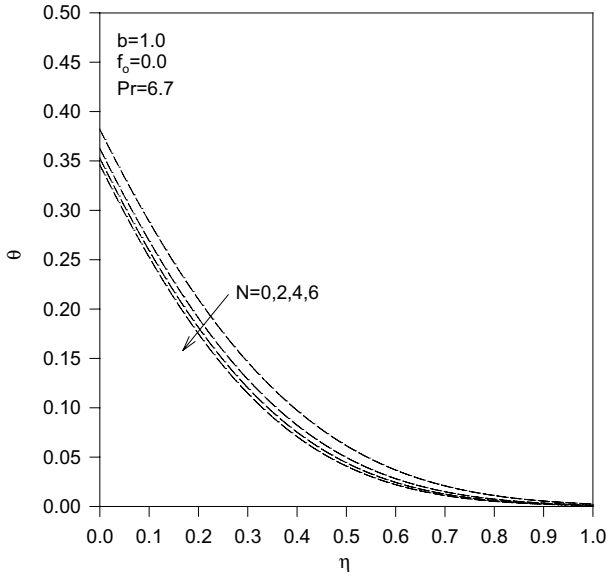

Fig. 3. Variations of θ with N.

noticed that the flow boundary layer thickness decreases as N increases causing the flow to be more attached to the horizontal surface. This causes an increase in the convective heat transfer coefficient. Thus, the surface temperature decreases as N increases which can be seen from Fig. 3.

Based on heat and mass transfer analogy with respect to chemical and biological applications, it is expected that the difference between analyte concentration at the microcantilever and the free stream concentration will decrease as N increases. Thus not only magnetic field can reduce flow instabilities inside thin film fluidic cells but it may also increase the detection capability of the sensor surface as for the microcantilever by increasing the analyte concentration near that surface. It is worth noting that the detection capability of the microcantilever is proportional to the analyte concentration near its active surface. On the other hand, the increase in the velocity of the analyte molecules near the sensor due to magnetic effects may decrease the binding rate at the sensor surface [6] since they will be in contact with the sensor surface for less time. Finally, cooling enhancements for the microcantilever become prominent as the Prandtl number increases as shown in Fig. 4.

Figs. 5 and 6 illustrate the effects of the wall dimensionless permeable velocity f_0 for permeable surfaces on both f' and θ, respectively. Suction conditions at the surface for negative f_0 values causes the flow to be more attached to the surface when compared with blowing conditions as shown in Fig. 5. Thus, surface cooling is enhanced under suction conditions as shown in Fig. 6. By heat and mass transfer analogy, it is expected that analyte concentration approaches free stream analyte concentration for suction conditions causing an enhancement in the sensor signal as discussed before. It is worth noting that suction conditions are achieved if the active surface of the sensor is opposing the disturbed boundary.

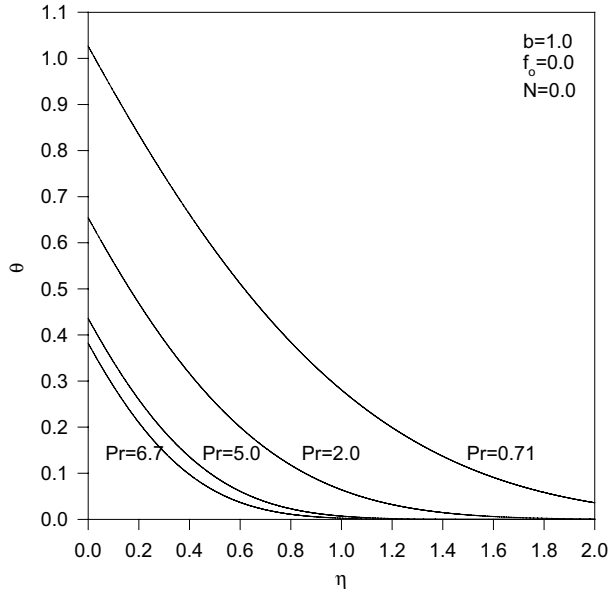

Fig. 4. Variations of θ with Pr.

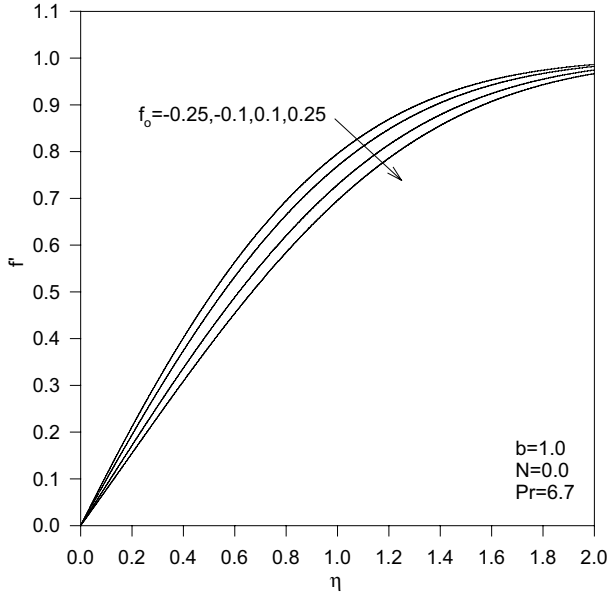

Fig. 5. Variations of f' with f_0.

4.1. Correlations

The correlations shown in Table 1 relate the local wall shear stress and the local Nusselt number that are found from the solution of Eqs. (8) and (9) to the controlling parameters b, N and Pr. All

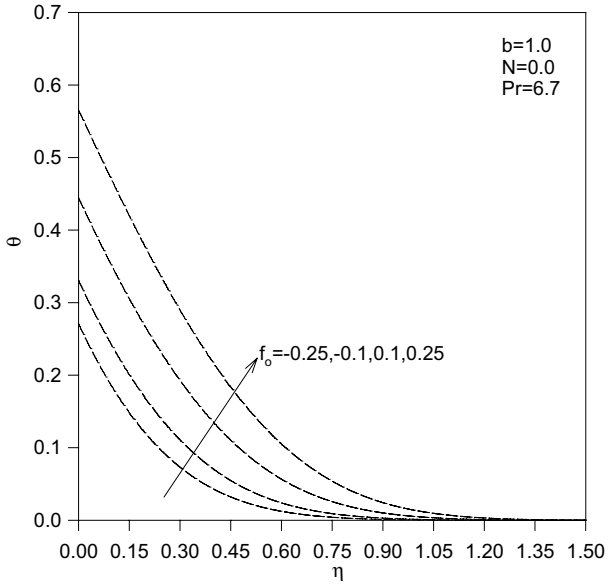

Fig. 6. Variations of θ with f_0.

Table 1
Correlations for local wall shear stress and local Nusselt number

Correlation	Range and maximum error
$\tau_w = 0.4565e^{-0.00717N}(1.0026+ 0.4684b - 0.0322b^2)\mu aRe^{1/2}$	$0.5 < b < 3.0$, $f_0 = 0$, $1 < N < 10$, Maximum error < 11%
$Nu = 1.174e^{0.00749N}\frac{Pr^{0.4566}}{b^{0.1919}}\left(\frac{x}{\sqrt{v(t+s/b)}}\right)$	
$\tau_w = 1.1973e^{(-0.7f_0-0.176b-0.103b^2)}\mu aRe^{1/2}$	$0.5 < b < 2.0$, $-0.2 < f_0 < 0.2$, $N = 0$, Maximum error < 12%
$Nu = 1.102e^{1.105f_0}Pr^{0.456}(0.689 + 0.294b)\left(\frac{x}{\sqrt{v(s+bt)}}\right)$	

the previous parameters have already been discussed except for "b". From the listed correlations, it can be seen that an increase in "b" causes reductions in both the local wall shear stress and the local Nusselt number. The reduction in "b" causes reductions in both the dimensionless velocity f' and temperature θ as shown in Figs. 7 and 8. It is worth noting that an increase in "b" causes a reduction in the squeezed free stream velocity. Finally, it worth noting similar trends in Figs. 3 and 6 can be obtained when the wall heat flux is considered to be uniform. In this case, the transformed energy equation, Eq. (9) or (13) need to be altered by eliminating the third term $(-f'\theta)$.

5. Conclusions

Flow and heat transfer over a horizontal permeable surface are analyzed in the presence of externally squeezed free stream, presence of a magnetic field normal to the flow and for permeable

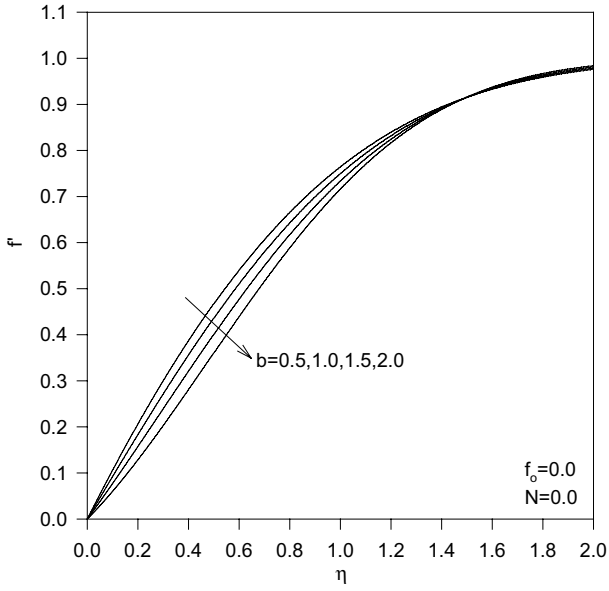

Fig. 7. Variations of f' with b.

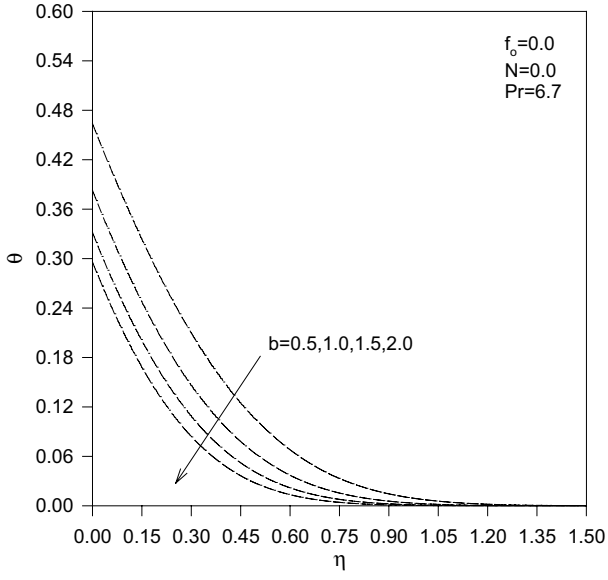

Fig. 8. Variations of θ with b.

surfaces. The corresponding unsteady boundary layer momentum and energy equations were transformed to similarity equations for certain families of the controlling parameters. Both local wall shear stress and local Nusselt numbers were found to increase as squeezing free stream

velocity increases. Further, local Nusselt number was increased by an increase in both the dimensionless magnetic parameter and the wall suction velocity. Further, the local wall shear stress was found to increase as the dimensionless magnetic parameter increases. Finally, hydromagnetic and suction wall permeable velocity effects were found to enhance the detection of the sensor as long as the chemical binding at the sensor surface is not suppressed by increases in flow associated with these effects.

Acknowledgement

We acknowledge support of this work by DOD/DARPA/DMEA under grant number DMEA90-02-2-0216.

References

[1] N.V. Lavrik, C.A. Tipple, M.J. Sepaniak, D. Datskos, Biomed. Microdev. 3 (1) (2001) 35–44.
[2] F.N. Ibrahim, M. Terbeche, J. Phys. D: Appl. Phys. 27 (1994) 740–747.
[3] T. Watanabe, I. Pop, Acta Mech. 105 (1994) 233–238.
[4] A.-R.A. Khaled, K. Vafai, Numer. Heat Transfer, Part A 43 (2003) 239–258.
[5] F.G. Blottner, AIAA J. 8 (1970) 193–205.
[6] W.F. Pritchard, P.F. Davis, Z. Derafshi, D.C. Polacek, R. Tsoa, R.O. Dull, S.A. Jones, D.P. Giddens, J. Biomech. 28 (1995) 1459–1469.